2022 2nd International Conference on Computers and Automation (CompAuto) | 978-1-6654-8194-6/22/$31.00 ©2022 IEEE | DOI: 10.1109/COMPAUTO55930.2022.00016

Pneumatic Artificial Muscle Antagonistic Joint Trajectory Tracking Using Adaptive Explicit Model Predictive Control

Kun Zhou
College of Mechanical and Electrical Engineering
China Jiliang University
Hangzhou 310018, China
13488950521@163.com

Xiaoyu Sun
College of Mechanical and Electrical Engineering
China Jiliang University
Hangzhou 310018, China
sunxiaoyuu163@163.com

Rui Yu
School of Electronic Information and Engineering
Tongji University
Shanghai 201804, China
fisherrui@163.com

Xiaolong Liu
Department of Mechanical Engineering
Johns Hopkins University
Baltimore, MD 21211, USA
xiaolong@jhu.edu

Binrui Wang*
College of Mechanical and Electrical Engineering
China Jiliang University
Hangzhou 310018, China
wangbrpaper@163.com

***Abstract*—In this paper, we present an explicit solution to adaptive model predictive control for a pneumatic artificial muscle (PAM) antagonistic joint trajectory tracking. Compared with the traditional model predictive control, the explicit model predictive control may pre-calculate the form of optimization solution offline, which saves the computation cost and reduce the time performance of the system. Meanwhile, we utilize an adaptive method to estimate the disturbance arbitrarily, instead of maximizing the disturbance directly. Finally, the simulation results and running time of the explicit adaptive model predictive control (EAMPC) method and the min-max model predictive control method are compared, which shows the efficiency of the proposed algorithm.**

Keywords—explicit solution, model predictive control, adaptive method, PAM, trajectory tracking

I. INTRODUCTION

With the development of pneumatic technology, the emergence, and application of new pneumatic components are increasing, and the PAM is one of the typical representatives. PAMs not only have the features of low cost, cleaning and easy installation but also own the advantages of high power/mass ratio, natural flexibility and mechanical characteristics which is similar to the biological muscles. Therefore, pneumatic actuators and other pneumatic structures [1]-[4] have become new research hotspots with practical research significance. And related research contents keep increasing in recent years.

Currently, the research on PAM mainly focuses on two directions: 1. Research on the model of PAM; 2. Research on the control of the PAM. The following is the introduction of the existing research results of PAMs. In terms of modeling, different modeling methods have been used to build PAM models. For example, a non-linear quasi-static model was developed to accurately capture actuation force versus contraction ratio behavior based on finite strain theory in [5]. Based on a nonlinear extended state observer in [6], the motion mechanism of the PAM was modeled as a dynamic nonlinear system. In the paper [7], the Bouc-Wen hysteresis model was modified to describe the asymmetric force/length hysteresis of the PAM, considering the effect of muscle length on hysteresis recovery. In the paper [8], a long short-term memory neural network model and an adaptive Takagi-Sugeno fuzzy model were proposed to represent the hysteretic relationship between PAMs displacement and fluid pressure. In terms of controlling, different control algorithms were also successfully applied to PAMs. For instance, the paper [9] presented an adaptive backstepping controller for a mechanism of pneumatic muscle actuators via an adaptive extended state observer. In the paper [10], an adaptive proxy-based sliding mode control approach was proposed for a class of typical second-order nonlinear systems. An efficient hysteresis compensation method based on the active modeling control was proposed in the paper [11], in order to improve the tracking accuracy of PAMs. And in [12], an advanced position-tracking control approach was proposed for a PAM system, referred to as an integrated intelligent nonlinear controller, Besides, the neural network algorithm was also applied in PAM, such as the paper [13], the author has proposed a neuroadaptive control method to deal with the uncertainty of nonlinear systems. At the same time, the paper [14]-[17] also conducted in-depth research on pneumatic muscles.

However, due to the limited range of expansion and contraction of the pneumatic muscle and the limited range of input of pneumatic valve, the above control algorithms are difficult to achieve a good control effect to the actual system. In view of the aforementioned reasons, we adopt a modified model

978-1-6654-8194-6/22/$31.00 ©2022 IEEE
DOI 10.1109/CompAuto55930.2022.00016

predictive control algorithm to control pneumatic muscle in this paper.

Model predictive control, since its launch in the 1970s, has developed into a new discipline branch with rich theory and practice content. Predictive control is aimed to optimize control problems and has been successful in complex industrial processes, which has fully displayed its potential for dealing with complex constrained optimization control. In recent years, there have been many achievements in solving the problem of constraint optimization control with model predictive control in many fields such as advanced manufacturing, energy, environment, aerospace, medical, etc. Besides, the theoretical research of model predictive control is becoming more and more mature. Such as the paper [18] studied adaptive model predictive control of systems with time-varying and potentially state-dependent uncertainties and proposes an estimation and prediction architecture within the min-max model predictive control framework. In [19], the author combined the enhanced single particle model with first-principles chemical/mechanical degradation physics to construct a new battery model to accurately predict dynamic intra-cycle capacity fade. And to improve the automation of the pre-cooling process, the author designed a model predictive control method based on Back-Propagation neural network as a surrogate inversion model in [20]. Meanwhile, the paper [21]-[25] described the latest research on model predictive control.

However, the traditional model predictive control algorithm is difficult to be implemented in small systems or embedded systems due to its characteristics of iterative update calculation which will lead to a huge computation. To reduce the amount of computation and speed up the running speed, we present an explicit solution to model predictive control for a PAM antagonistic joint trajectory tracking in this paper. Explicit model predictive control [26]-[28] is a fast model predictive control algorithm proposed by Bemporad in 2002 [29]. The main idea of the explicit predictive control algorithm is to pre-calculate optimization solution off-line through the idea of multiparametric programming in order to improve the speed of online calculation and make the system have better real-time performance. In this case, the model predictive control can be applied to the system with high sampling frequency and high real-time requirement. Applying the explicit model predictive control algorithm to the control of PAM joint trajectory tracking can not only achieve the optimal control effect but also improve the real-time performance of the system. In addition, we will estimate the disturbance adaptively.

The main contributions of the paper are summarized as follows: (1) Establish and discretize of PAM model, which enables the model to be processed explicitly. (2) Propose the adaptive estimator to estimate the disturbance. (3) Apply the EAMPC algorithm to a tracking problem of PAM joint, which may optimize control inputs and limits the range of inputs and state variables.

The structure of the paper is organized as follows. In section 2, we model the PAM with disturbance. In section 3, we deal with the uncertain disturbance by using the adaptive method and discretize the model. In section 4, we apply the EAMPC algorithm for the PAM system trajectory tracking analysis. In addition, the simulation result is shown in section 5 and the conclusion of this paper is given in section 6.

II. Model and Problem Statement

The control diagram of the PAM antagonistic joint is shown in Fig. 1. And the modeling process of the joint, such as [9], can be obtained as follows.

$$\begin{aligned} u_1(t) &= u_0 + k_u u(t) \\ u_2(t) &= u_0 - k_u u(t) \end{aligned} \tag{1}$$

where k_u is a voltage coefficient, u_0 is an initial voltage, $u_1(t)$ and $u_2(t)$ are respectively two input control voltages of pressure proportional valves and $u(t)$ is the control law of this system.

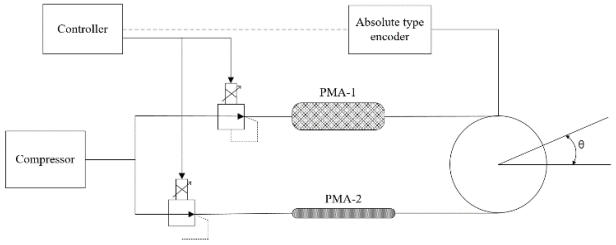

Fig. 1. Control circuit diagram of pneumatic muscle joint

There is a certain proportion of the input control voltages and the output pressures of the pressure proportional valves and the proportional coefficient is k_0, from which we can obtain the following equation.

$$\begin{aligned} P_1(t) &= P_0 + \Delta P(t) = k_0 u_1(t) \\ P_2(t) &= P_0 - \Delta P(t) = k_0 u_2(t) \end{aligned} \tag{2}$$

where P_0 is the initial pressure of PMAs, $\Delta P(t)$ is the pressure difference, $P_1(t)$ and $P_2(t)$ are two internal pressures of PMAs.

The mathematical model of pneumatic muscle [9] is established as follows.

$$\begin{aligned} F_1(t) &= P_1(t)\left(k_1\varepsilon_1(t)^2 + k_2\varepsilon_1(t) + k_3\right) + k_4 \\ F_2(t) &= P_2(t)\left(k_1\varepsilon_2(t)^2 + k_2\varepsilon_2(t) + k_3\right) + k_4 \end{aligned} \tag{3}$$

where F_1 and F_2 are two pulling forces of PMAs, k_1, k_2, k_3 and k_4 are parameters for the mathematical models of PMAs, $\varepsilon_1(t)$ and $\varepsilon_2(t)$ are two shrinking rates which are ratios of contraction lengths and initial lengths for PMAs.

$$\begin{aligned} \varepsilon_1(t) &= \varepsilon_0 + rL_0^{-1}\theta(t) \\ \varepsilon_2(t) &= \varepsilon_0 - rL_0^{-1}\theta(t) \end{aligned} \tag{4}$$

where ε_0 and L_0 are the initial shrinking rate and initial length for PMAs, and r is the gear radius of the joint.

According to the kinematic model of pneumatic muscle joints, the following equation can be obtained.

$$T(t)=J\ddot{\theta}(t)+b_v\dot{\theta}(t)=F_1(t)d_1-F_2(t)d_2+\vartheta(t) \tag{5}$$

where J represents the inertia moment of PMAs, b_v represents the coefficient of damping, $\vartheta(t)$ indicates an unknown term such as external disturbances and unmodeled dynamics for the mechanism of PMAs. And let $d_1=d_2=r$. Substituting (2), (3) and (4) into (5), we can rewrite (5) as follows

$$\begin{aligned}T(t)&=k_0u_0r\left(4k_1\varepsilon_0rL_0^{-1}+2k_2rL_0^{-1}\right)\theta(t)\\&\quad+k_0k_urMu(t)+\vartheta(t)\\M&=2k_1\varepsilon_0^2+2k_1\left(r\theta(t)L_0^{-1}\right)^2+2k_2\varepsilon_0+2k_3\end{aligned} \tag{6}$$

where $2k_1(r\theta(t)L_0^{-1})^2u(t)$ is considered in the unknown term $\vartheta(t)$. Then the dynamic model can be rewritten as

$$\begin{aligned}\ddot{\theta}(t)&=-\frac{b_v}{J}\dot{\theta}(t)+\frac{2k_0u_0r^2\left(2k_1\varepsilon_0+k_2\right)L_0^{-1}}{J}\theta(t)\\&\quad+\frac{2k_0k_ur\left(k_1\varepsilon_0^2+k_2\varepsilon_0+k_3\right)}{J}u(t)+d(t)\end{aligned} \tag{7}$$

Select the state of the system, let

$$x_1(t)=\theta(t),\ x_2(t)=\dot{\theta}(t) \tag{8}$$

The dynamic system of pneumatic muscle joint can be expressed as follows

$$\begin{aligned}\dot{x}_1(t)&=x_2(t)\\\dot{x}_2(t)&=b_1x_1(t)+b_2x_2(t)+d(t)+bu(t)\\y(t)&=x_1(t)\end{aligned} \tag{9}$$

where $y(t)$ is the output of the system, and

$$\begin{aligned}b&=\frac{2k_0k_ur\left(k_1\varepsilon_0^2+k_2\varepsilon_0+k_3\right)}{J}\\b_1&=\frac{2k_0u_0r^2\left(2k_1\varepsilon_0+k_2\right)L_0^{-1}}{J}\\b_2&=-\frac{b_v}{J}\\d(t)&=\frac{\vartheta(t)}{J}\end{aligned}$$

The parameters of b, b_1, b_2 are known, and $d(t)$ is the unknown term associated with states. Because the purpose of our control is trajectory tracking, we may need the assumption about the reference signal as follow:

A. Assumption 2.1

The reference signal is y_r, and y_r is a constant in this paper. Now, we consider the model of the PAM as:

$$\begin{aligned}\dot{x}(t)&=\mathbf{A}x(t)+\mathbf{B}u(t)+\delta\left(t,x(t)\right)\\y(t)&=\mathbf{C}x(t)\\x(t_0)&=x(0)\end{aligned} \tag{10}$$

where

$$\mathbf{A}=\begin{bmatrix}0&1\\b_1&b_2\end{bmatrix},\ \mathbf{B}=\begin{bmatrix}0\\b\end{bmatrix},\ \mathbf{C}=\begin{bmatrix}1&0\end{bmatrix}$$

and the system state $x\in\chi\subset R^2$, the control input $u\in U\subset R^1$, $\chi\times U\to R^2$ is a known function, and $\delta\in\chi$ is the unknown disturbance.

Note that we can get the value of x from the actual system. Suppose $f(x,u)$ is local Lipchitz that satisfies

$$\begin{aligned}&\|\mathbf{A}x+\mathbf{B}u-\mathbf{A}y-\mathbf{B}v\|\le l_x\|x-y\|+l_u\|u-v\|\\&\|\mathbf{A}x+\mathbf{B}u\|\le l_x\|x\|+l_u\|u\|\\&x,y\in\chi,v\in U\end{aligned} \tag{11}$$

where l_x, l_u are positive constant. Then, let's assume that $\delta\left(t,x(t)\right)$ satisfies the following condition.

B. Assumption 2.2

The reference signal is y_r, and y_r is a constant in this paper. Now, we consider the model of the PAM as:

$$\begin{aligned}&\|\delta(t,x)-\delta(\tau,y)\|\le l_\delta\|x-y\|+l_t|t-\tau|\\&\|\delta(t,0)\|\le b_\delta\\&\left\|\frac{\partial\delta(t,x)}{\partial t}\right\|\le l_{\delta_t}\|x\|+b_{\delta_t}\\&\left\|\frac{\partial\delta(t,x)}{\partial t}\right\|\le l_{\delta_x}\|x\|+b_{\delta_x}\\&x,y\in\chi,\ |t-\tau|\le T,\forall t\ge0\end{aligned}$$

where T is a positive constant, and have positive parameters l_δ, l_t, b_δ, l_{δ_t}, b_{δ_t}, l_{δ_x}, b_{δ_x} that satisfy above inequalities.

Meanwhile, when $t=\tau$, $y=0$, we can obtain the following inequality:

$$\begin{aligned}&\|\delta(\tau,x)-\delta(\tau,0)\|+\|\delta(\tau,0)\|\le l_\delta\|x\|+b_\delta\\&\|\delta(\tau,x)\|\le l_\delta\|x\|+b_\delta\end{aligned}$$

From Assumption 2.2, we can define a constant β and a set Ω as

$$\beta=l_\delta\max_{x\in\chi}\|x\|+b_\delta,\Omega=\left\{\omega\in R^2\mid\|\omega\|\le\beta\right\} \tag{12}$$

Therefore, we can obtain $\delta(t,x(t))\in\Omega$ for $\forall t\ge0$.

The purpose of this paper is to find the explicit solution for the trajectory tracking of the pneumatic muscle joint system with constrained state and input. We will choose the EAMPC approach to solve this problem. We need to set a time sequence as $t_k=kT$, $t_0=0$, $k\in N$ where T is the sampling period, which is for sampling the states x from real system. And we will solve the constrained optimal control problem over the time interval $\left[t_k,t_{k+N}\right)$, $t_{k+N}=(k+N)T\ge kT$. Now, we can present the problem in discrete-time as

Problem 1.

$$\min_{u\in U} J\left(u \mid x\left(t_k\right)\right)$$

$$\begin{aligned} s.t. \quad & \bar{x}_k^{i+1} = \mathbf{A}^* \bar{x}_k^i + \mathbf{B}^* u_k^i + \Delta_k, \bar{x}_k^0 = x\left(t_k\right) \\ & \bar{y}_k^{i+1} = \mathbf{C}\bar{x}_k^i \\ & \bar{x}_k^i \in \chi - \left\|\epsilon^i\right\|, u_k^i \in U, i \in [0, N] \end{aligned}$$

$$J\left(u \mid x\left(t_k\right)\right) = \sum_{i=0}^{N} Q\left(\bar{y}_k^i - r\right)^2 + \sum_{i=0}^{N-1} R\left(u_k^i\right)^2$$

where Q, R are positive constants.

In the next section, we will give a detailed explanation of A^*, B^*, Δ_k and $\chi - \left\|\epsilon^i\right\|$ in the problem 1.

III. Problem Fprmulation

A. Adaptive Estimation

In this section, we are going to estimate the uncertainty $\delta(t,x(t))$ using the adaptive method like [18]. An adaptive estimator is defined as:

$$\begin{aligned} \dot{z}\left(t\right) &= -a\tilde{x}\left(t\right) + \mathbf{A}x + \mathbf{B}u + \hat{\sigma}\left(t\right) \\ z\left(0\right) &= x_0 \end{aligned} \tag{13}$$

where z is the estimate of state, $\tilde{x}\left(t\right) = z\left(t\right) - x\left(t\right)$ is the estimate error of state, and a a is an arbitrarily chosen positive parameter. Meanwhile, $\hat{\sigma}\left(t\right)$ is updated by the adaptation law as following:

$$\begin{aligned} \hat{\sigma}\left(t\right) &= -\Phi\left(T\right)\tilde{x}\left(kT\right),\ \hat{\sigma}\left(0\right) = 0 \\ \Phi\left(T\right) &= \frac{a}{e^{aT} - 1} \end{aligned} \tag{14}$$

where $t \in \left[kT, (k+1)T\right)$, $k = 0,1,2...$ and T is the sampling time.

Remark 1.

The adaptive estimator proposed in (13)-(14) is extended by the piecewise-constant adaptive law in literature [30]. Reference to [18], from (13) and (14), the performance of this estimator is established by the lemma as following:

Lemma 3.1.

Under the Assumption 2.2 is satisfied, when $t = t_k$, we can obtain the inequality

$$\left\|\delta\left(t_k, x\left(t_k\right)\right) - \hat{\sigma}\left(t_k\right)\right\| \le \phi\left(x\left(t_k\right), t - t_k\right) \tag{15}$$

satisfied for $\forall t \ge 0$, where

$$\begin{aligned} \phi\left(x\left(t_k\right), t - t_k\right) &= l_\delta \left(\left\|x\left(t_k\right)\right\| + \frac{\varepsilon}{l_x + l_\delta} \right) \left(e^{\left(l_x + l_\delta\right)\left(t - t_k\right)} - 1 \right) \\ &\quad + l_t\left(t - t_k\right) + \gamma\left(T\right) \\ \gamma\left(T\right) &= 2rT + \left\|1 - e^{-aT}\right\| \beta \end{aligned}$$

$$\begin{aligned} r = {} & l_{\delta_t} \max_{x\in\chi} \|x\| + b_{\delta_t} \\ & + \left(l_{\delta_x} \max_{x\in\chi} \|x\| + b_{\delta_x} \right) \left(\max_{x\in\chi, u\in U} \|\mathbf{A}x + \mathbf{B}u\| + \beta \right) \end{aligned}$$

where β is defined in (12).

Remark 2.

The adaptive estimator proposed in (13)-(14) is extended by the piecewise-constant adaptive law in literature [30]. Reference to [18], from (13) and (14), the performance of this estimator is established by the lemma as following:

It can be seen from the above formula that, as long as the sampling time T is small enough, the estimation error bound $\gamma(T)$ can be arbitrarily small. Which means that the estimation accuracy of the disturbance depends on the hardware of the system.

It can be seen from the above formula that, as long as the sampling time T is small enough, the estimation error bound $\gamma(T)$ can be arbitrarily small. Which means that the estimation accuracy of the disturbance depends on the hardware of the system.

From (11) and Assumption 2.2, and let $\varepsilon = l_u \max_{u\in U} \|u\| + b_\delta$, we can get following inequalities is the same as [18]:

$$\begin{aligned} & \left\|\delta\left(t, x\left(t\right)\right) - \delta\left(t_k, x\left(t_k\right)\right)\right\| \\ & \le l_\delta \left(\left\|x\left(t_k\right)\right\| + \frac{\varepsilon}{l_x + l_\delta} \right) \left(e^{\left(l_x + l_\delta\right)\left(t - t_k\right)} - 1 \right) + l_t\left(t - t_k\right) \end{aligned} \tag{16}$$

Finally, based on (15) and (16), we can obtain that

$$\begin{aligned} & \left\|\delta\left(t, x\left(t\right)\right) - \hat{\sigma}\left(t_k\right)\right\| \\ & \le \left\|\delta\left(t, x\left(t\right)\right) - \delta\left(t_k, x\left(t_k\right)\right)\right\| + \left\|\delta\left(t_k, x\left(t_k\right)\right) - \hat{\sigma}\left(t_k\right)\right\| \\ & \le l_\delta \left(\left\|x\left(t_k\right)\right\| + \frac{\varepsilon}{l_x + l_\delta} \right) \left(e^{\left(l_x + l_\delta\right)\left(t - t_k\right)} - 1 \right) + l_t\left(t - t_k\right) + \gamma\left(T\right) \\ & = \phi\left(x\left(t_k\right), t - t_k\right) \end{aligned} \tag{17}$$

where $\phi(x(t_k), t - t_k)$ is a constant that can be chosen arbitrarily.

Therefore, we can substitute $\delta(t,x(t))$ using $\hat{\sigma}(t_k)$, then (10) can be rewritten as

$$\begin{aligned} \dot{\bar{x}}\left(t\right) &= \mathbf{A}\bar{x}\left(t\right) + \mathbf{B}u\left(t\right) + \hat{\sigma}\left(t_k\right) \\ \bar{y}\left(t\right) &= \mathbf{C}\bar{x}\left(t\right) \\ \bar{x}\left(t_k\right) &= x\left(t_k\right),\ t \in \left(t_k, t_{(k+N)}\right] \end{aligned} \tag{18}$$

B. States Constraints

In the prediction process, we have to satisfy the condition of $x(t) \in \chi$. However, at the kth computation, the establishment of $\bar{x}^1 = \bar{x}_k(t_{k+1}) \in \chi$ can not guarantee the establishment of $x(t_{k+1}) \in \chi$ due to the error between $\bar{x}(t)$ and $x(t)$. Therefore, to ensure $x(t) \in \chi$, we have to make a reduced set $\bar{\chi}$ from χ. The detailed process as follows:

Theorem 3.1.

The adaptive estimator proposed in (13)-(14) is extended by the piecewise-constant adaptive law in literature [30]. Reference to [18], from (13) and (14), the performance of this estimator is established by the lemma as following:

Let $\bar{\epsilon} = \bar{x}(t) - x(t)$, and we can get

$$\|\bar{\epsilon}\| \le \frac{1}{l_x}\phi\left(x(t_k), t_N - t_k\right)\left(e^{l_x(t-t_k)} - 1\right)$$

We can obtain the feasibility set of $\bar{x}(t) \in \bar{\chi} = \chi - \|\bar{\epsilon}\|$.

Proof:

The derivative of $\bar{\epsilon}$ is

$$\begin{aligned}\dot{\bar{\epsilon}} &= \dot{\bar{x}}(t) - \dot{x}(t)\\ &= \mathbf{A}\bar{x}(t) + \mathbf{B}u(t) + \hat{\sigma}(t_k) - \mathbf{A}x(t) - \mathbf{B}u(t) - \delta(t, x(t))\end{aligned}$$

Based on (17), the following inequality can be obtain

$$\begin{aligned}&\frac{d}{dt}\|\bar{\epsilon}\| \le \|\dot{\bar{\epsilon}}\|\\ &= \left\|\mathbf{A}\bar{x}(t) + \mathbf{B}u(t) + \hat{\sigma}(t_k) - \mathbf{A}x(t) - \mathbf{B}u(t) - \delta(t, x(t))\right\|\\ &\le \left\|\left(\mathbf{A}\bar{x}(t) + \mathbf{B}u(t)\right) - \left(\mathbf{A}x(t) + \mathbf{B}u(t)\right)\right\| + \left\|\hat{\sigma}(t_k) - \delta(t, x(t))\right\|\\ &\le l_x\left\|\bar{x}(t) - x(t)\right\| + \phi\left(x(t_k), t - t_k\right)\\ &= l_k\|\bar{\epsilon}\| + \phi\left(x(t_k), t - t_k\right)\end{aligned}$$

Then we can obtain

$$\|\bar{\epsilon}\| \le \frac{1}{l_x}\phi\left(x(t_k), t_N - t_k\right)\left(e^{l_x(t-t_k)} - 1\right)$$

which completes the proof. And the feasible set of $\bar{x}(t)$ by using $\hat{\sigma}(t)$ can be expressed as

$$\begin{aligned}&\bar{x}(t) \in \chi - \|\bar{\epsilon}\|, t \in (t_k, t_{k+N}]\\ &\|\bar{\epsilon}\| \le \frac{1}{l_x}\phi\left(x(t_k), t_N - t_k\right)\left(e^{l_x(t-t_k)} - 1\right)\end{aligned} \tag{19}$$

C. Model Discretization

In this subsection, we need to discretize the PAM system model (18). The discrete equation is shown below

$$\begin{aligned}\bar{x}_k^{i+1} &= e^{\mathbf{A}T}\bar{x}_k^i + \mathbf{A}^{-1}\left(e^{\mathbf{A}T} - 1\right)\mathbf{B}u_k + \mathbf{A}^{-1}\left(e^{\mathbf{A}T} - 1\right)\hat{\sigma}(t_k)\\ \bar{y}_k^{i+1} &= \mathbf{C}\bar{x}_k^i\end{aligned} \tag{20}$$

Let

$$\begin{aligned}\mathbf{A}^* &= e^{\mathbf{A}T}\\ \mathbf{B}^* &= \mathbf{A}^{-1}\left(e^{\mathbf{A}T} - 1\right)\mathbf{B}\\ \mathbf{\Delta}_k &= \mathbf{A}^{-1}\left(e^{\mathbf{A}T} - 1\right)\hat{\sigma}(t_k)\end{aligned}$$

Then (20) can be rewritten as

$$\begin{aligned}\bar{x}_k^{i+1} &= \mathbf{A}^*\bar{x}_k^i + \mathbf{B}^*u_k^i + \mathbf{\Delta}_k\\ \bar{y}_k^{i+1} &= \mathbf{C}\bar{x}_k^i\end{aligned} \tag{21}$$

where $\mathbf{A}^*$, $\mathbf{B}^*$ and $\mathbf{\Delta}_k$ are constant matrices.

And the feasible set combining with (19) should be defined to be

$$\begin{aligned}&\bar{x}(t) \in \bar{\chi} = \chi - \|\bar{\epsilon}^i\|, i \in [0, N]\\ &\|\bar{\epsilon}^i\| = \frac{1}{l_x}\phi\left(x(t_k), t_N - t_k\right)\left(e^{l_x(iT)} - 1\right)\end{aligned} \tag{22}$$

IV. EAMPC Trajectory

In this section, we will solve Problem 1 by using KKT conditions and get the optimized control input u by solving a mpQP (multi-parametric quadratic programming) problem. Because we can always get $\bar{y}_k^i - r = \mathbf{C}\bar{x}_k^i - r$ only in terms of $\bar{x}_k^0$ and $U = [u_k^0, ..., u_k^{N-1}]$, we can represent the summing function as

$$\begin{aligned}J\left(u|x(t_k)\right) = {}& \mathbf{X}_k^T\mathbf{M}\mathbf{X}_k + \mathbf{U}^T\mathbf{G}\mathbf{U} + \mathbf{U}^T R\mathbf{U} + \mathbf{\Gamma}_k^T\mathbf{J}\mathbf{\Gamma}_k + 2\mathbf{\Gamma}_k^T\mathbf{K}\mathbf{X}_k\\ &+ 2\mathbf{\Gamma}_k^T\mathbf{H}\mathbf{U} + 2\mathbf{X}_k^T\mathbf{W}\mathbf{U} - 2rQ\mathbf{N}\mathbf{U} - 2rQ\mathbf{P}\mathbf{\Gamma}_k\\ &- 2rQ\mathbf{S}\mathbf{X}_k + Q\left(\mathbf{C}\bar{x}_k^0\right)^2 - 2QR\left(\mathbf{C}\bar{x}_k^0\right) + (\mathbf{N}+1)Qr^2\end{aligned}$$

where

$$\begin{aligned}&\mathbf{N} = \tau\mathbf{D}, \mathbf{P} = \tau\mathbf{E}, \mathbf{S} = \tau\mathbf{F}\\ &\mathbf{G} = Q\mathbf{N}^T\mathbf{N}, \mathbf{M} = Q\mathbf{S}^T\mathbf{S}, \mathbf{J} = Q\mathbf{P}^T\mathbf{P}\\ &\mathbf{H} = Q\mathbf{P}^T\mathbf{H}, \mathbf{W} = Q\mathbf{N}^T\mathbf{S}, \mathbf{K} = Q\mathbf{P}^T\mathbf{S}\end{aligned}$$

and

$$\mathbf{F} = \begin{bmatrix}\mathbf{A}^* & 0 & ... & 0\\ 0 & \mathbf{A}^{*2} & ... & 0\\ . & . & ... & .\\ . & . & ... & .\\ 0 & 0 & ... & \mathbf{A}^{*N}\end{bmatrix},\ \mathbf{X}_k = \begin{bmatrix}\bar{x}_k^0\\ \bar{x}_k^0\\ .\\ .\\ .\\ \bar{x}_k^0\end{bmatrix}$$

$$\mathbf{D} = \begin{bmatrix}\mathbf{B}^* & 0 & ... & 0\\ \mathbf{A}^*\mathbf{B}^* & \mathbf{B}^* & ... & 0\\ . & . & ... & .\\ . & . & ... & .\\ \mathbf{A}^{*(N-1)}\mathbf{B}^* & \mathbf{A}^{*(N-2)}\mathbf{B}^* & ... & \mathbf{B}^*\end{bmatrix}$$

$$\mathbf{E} = \begin{bmatrix}\mathbf{I} & 0 & ... & 0\\ \mathbf{A}^* & \mathbf{I} & ... & 0\\ . & . & ... & .\\ . & . & ... & .\\ \mathbf{A}^{*(N-1)} & \mathbf{A}^{*(N-2)} & ... & \mathbf{I}\end{bmatrix}$$

$$\mathbf{U} = \begin{bmatrix}u_k^0\\ u_k^1\\ .\\ .\\ .\\ u_k^{N-1}\end{bmatrix}, \mathbf{\Gamma}_k = \begin{bmatrix}\mathbf{\Delta}_k\\ \mathbf{\Delta}_k\\ .\\ .\\ .\\ \mathbf{\Delta}_k\end{bmatrix}, \tau = \begin{bmatrix}\mathbf{C}\\ \mathbf{C}\\ .\\ .\\ .\\ \mathbf{C}\end{bmatrix}$$

Now, let's assume the boundary condition for the states as following

$$\bar{x}_k^i \le v_k$$

where $v_k (k = 1,2)$ is the boundary of the states, then it can be expressed as

$$\mathbf{F}\mathbf{X}_k + \mathbf{D}\mathbf{U} + \mathbf{E}\boldsymbol{\Gamma}_k \le \mathbf{V}$$

where

$$\mathbf{V} = [v_1, v_2]^T$$

Then, as [13], we can get the KKT conditions as follows:

$$\nabla_u L = 2\mathbf{W}^T\mathbf{X}_k + 2\mathbf{H}^T\boldsymbol{\Gamma}_k + 2\mathbf{G}\mathbf{U} + 2R\mathbf{U} - 2\mathbf{N}^T + \mathbf{D}^T\lambda = 0$$

$$\lambda_j\left(\mathbf{V}_j - \mathbf{F}_j\mathbf{X}_k - \mathbf{D}_j\mathbf{U} - \mathbf{E}_j\boldsymbol{\Gamma}_k\right) = 0, j = 1,2$$

$$\mathbf{F}\mathbf{X}_k + \mathbf{D}\mathbf{U} + \mathbf{E}\boldsymbol{\Gamma}_k - \mathbf{V} \le 0$$

$$\lambda_j \ge 0, \lambda \in R^2$$

For inactive constraints, we can obtain

$$2\hat{\mathbf{W}}^T\mathbf{X}_k + 2\hat{\mathbf{H}}^T\boldsymbol{\Gamma}_k + 2\hat{\mathbf{G}}\mathbf{U} + 2R\mathbf{U} - 2\hat{\mathbf{N}}^T = 0$$

where $\hat{\mathbf{W}}$, $\hat{\mathbf{H}}$, $\hat{\mathbf{G}}^{-1}$, $\hat{\mathbf{N}}$ are constructed by the rows in original matrices when $\lambda_j = 0$.

For active constraints, we can get

$$\tilde{\mathbf{V}} - \tilde{\mathbf{C}}\mathbf{X}_k - \tilde{\mathbf{G}}\mathbf{U} - \tilde{\mathbf{J}}\boldsymbol{\Gamma}_k = 0$$

where $\tilde{\mathbf{V}}$, $\tilde{\mathbf{C}}$, $\tilde{\mathbf{G}}^{-1}$, $\tilde{\mathbf{J}}$ are constructed by the rows in original matrices when $\lambda_j \ne 0$.

Then the optimized problem can be presented as

$$\begin{bmatrix} 2\hat{\mathbf{W}}^T \\ -\tilde{\mathbf{C}} \end{bmatrix}\mathbf{X}_k + \begin{bmatrix} 2\hat{\mathbf{G}} + 2R \\ -\tilde{\mathbf{G}} \end{bmatrix}\mathbf{U} + \begin{bmatrix} 2\hat{\mathbf{H}}^T \\ -\tilde{\mathbf{J}} \end{bmatrix}\boldsymbol{\Gamma}_k + \begin{bmatrix} -2\hat{\mathbf{N}}^T \\ \tilde{\mathbf{V}} \end{bmatrix} = 0$$

Therefore, we can solve the optimization problem as

$$\mathbf{U} = \begin{bmatrix} -2\hat{\mathbf{G}} - 2R \\ \tilde{\mathbf{G}} \end{bmatrix}^{-1}\left(\begin{bmatrix} 2\hat{\mathbf{W}}^T \\ -\tilde{\mathbf{C}} \end{bmatrix}\mathbf{X}_k + \begin{bmatrix} 2\hat{\mathbf{H}}^T \\ -\tilde{\mathbf{J}} \end{bmatrix}\boldsymbol{\Gamma}_k + \begin{bmatrix} -2\hat{\mathbf{N}}^T \\ \tilde{\mathbf{V}} \end{bmatrix}\right)$$

Finally, we can express the EAMPC Algorithm as follows

EAMPC ALGORITHM

Solve the mpQP offline: Get the optimized input $[u_k^0]^*$ in terms of by $\bar{x}_k^0$ and $\hat{\sigma}(t_k)$.
At time t_0: Start running the estimator defined as (13).
At time $t = t_k$: 1. Compute $\hat{\sigma}(x_k)$ according to (14); 2. Insert $x(t_k)$ and $\hat{\sigma}(x_k)$ to offline optimizer; 3. Get the optimized input $u(t)^*$ for $t \in [t_k, t_{k+1})$ and use it to the plant.

V. SIMULATION

This section presents the matlab simulation experiments that demonstrate the performance of the proposed EAMPC algorithm for a PAM antagonistic joint with disturbance. In the simulation, the parameters of PAM antagonistic joint are taken as following Table I:

TABLE I. THE SYSTEM PARAMETERS OF PAM

k_0	k_u	k_1	k_2	k_3	r	ε_0	L_0
0.09	0.45	10	7.5	1.6	0.25	0.1	0.2

In order to display the effect of the proposed algorithm more intuitively, we compared the simulation results of the EAMPC algorithm with the min-max model predictive control algorithm. Two sets of experiments as follows:

Case 1:

In the first simulation, the initial values are chosen to be $x_1 = 0$, $x_2 = -1$, $u_0 = 2$, disturbance is chosen as $d(t) = \sin(x_1 + x_2)$ which is dependent of the states, and the tracking signal is $y_r = 1$.

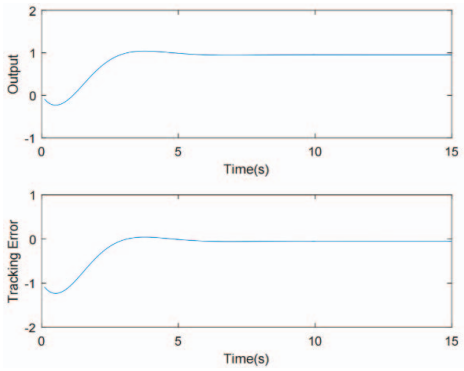

Fig. 2. The output and tracking error trajectory generated by EAMPC

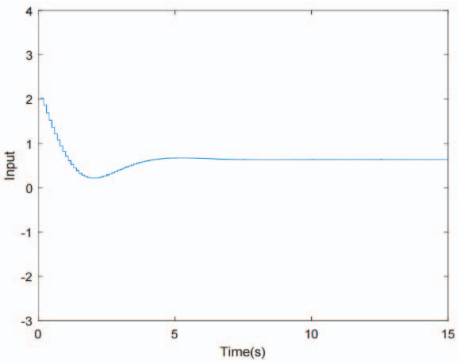

Fig. 3. The input trajectory generated by EAMPC

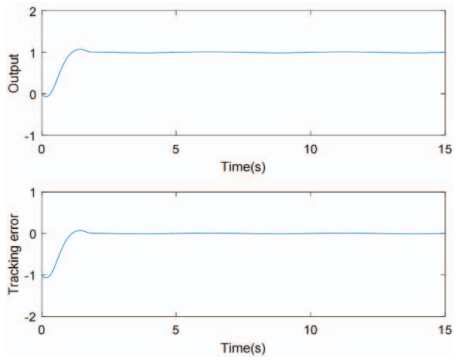

Fig. 4. The output and tracking error trajectory generated by min-max model predictive control

Fig. 2 shows the output trajectory and tracking error trajectory, and Fig. 3 shows the input trajectory generated by EAMPC. For comparison, the output trajectory and tracking error trajectory are given in Fig. 4, and the input trajectory is given in Fig. 5 generated by min-max model predictive control.

TABLE II. RUNNING TIME OF TWO ALGORITHMS

t_{EAMPC}	6.58	6.69	6.65	7.05	6.64
$t_{\min-\max MPC}$	161.57	161.45	161.37	164.05	161.12

Meanwhile, we carried out five groups comparison of the two algorithms, and the running time is shown respectively in Table II.

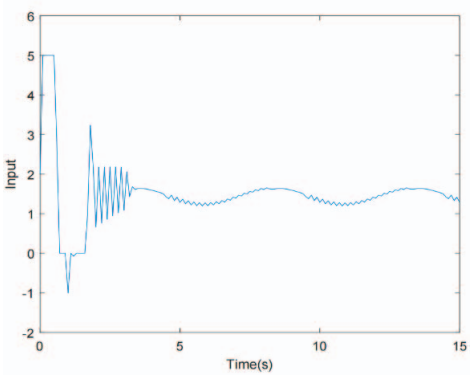

Fig. 5. The input trajectory generated by min-max model predictive control

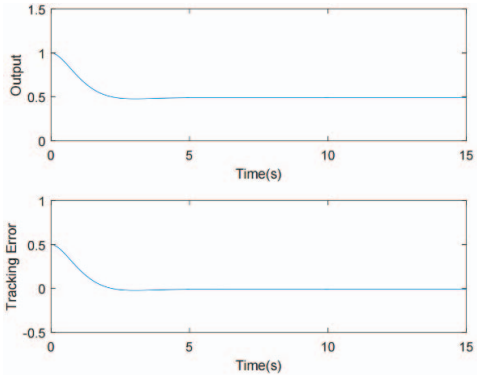

Fig. 6. The output and tracking error trajectory generated by EAMPC

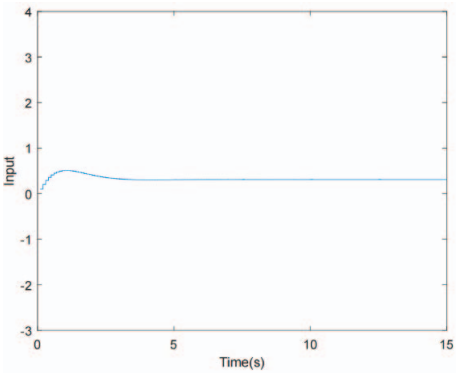

Fig. 7. The input trajectory generated by EAMPC

Case 2:

In the second simulation, the initial values are chosen to be $x_1 = 1$, $x_2 = 0$, $u_0 = 0$, disturbance is chosen as $d(t) = 0.5\cos(x_1 + x_2)$ which is dependent of the states, and the tracking signal is $y_r = 0.5$. Fig. 6 shows the output trajectory and tracking error trajectory, and Fig. 7 shows the input trajectory generated by EAMPC. For comparison, the output trajectory and tracking error trajectory is given in Fig. 8, and the input trajectory is given in Fig. 9 generated by min-max model predictive control.

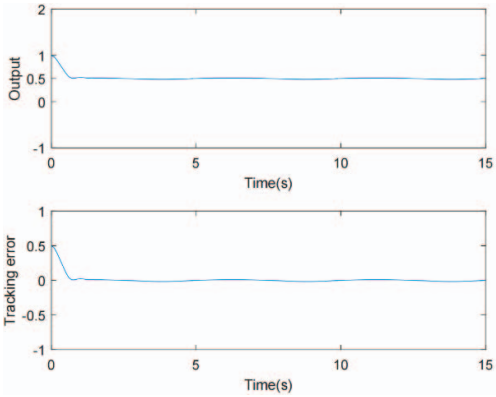

Fig. 8. The output and tracking error trajectory generated by min-max model predictive control

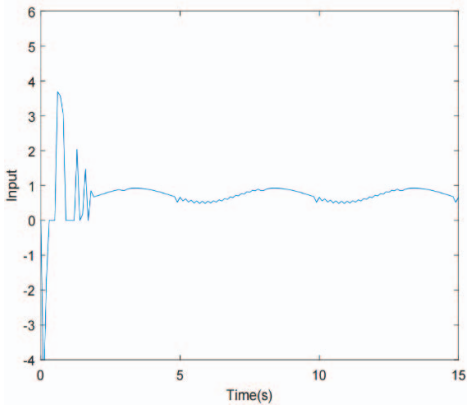

Fig. 9. The input trajectory generated by min-max EAMPC

Also, we carried out five groups comparison of the two algorithms, and the running time is shown respectively in Table III.

TABLE III. RUNNING TIME OF TWO ALGORITHMS

t_{EAMPC}	6.57	6.68	6.66	6.58	6.65
$t_{\min-\max MPC}$	159.17	159.45	158.85	160.16	159.44

Comparing the result figures of the two algorithms, we can obtain that the input signal of the EAMPC algorithm is smoother and lower. And from the results of running time, it is shown that the EAMPC algorithm can effectively improve the running speed of the system and reduce the running time on the

premise of ensuring the stability and tracking the performance of the system.

VI. Conclusion

An explicit solution to adaptive model predictive control for a PAM antagonistic joint trajectory tracking has been presented in this paper. We consider the model with a time-varying disturbance and design an adaptive estimator to estimate it. Also, the feasibility of the system ensured the EAMPC algorithm. In addition, the simulation studies not only verify the effectiveness of the proposed control scheme but also effectively prove the EAMPC algorithm can improve running time by comparing with the min-max model predictive control algorithm. For further research, we are going to consider the situation that the parameters of the system are unknown.

References

[1] Sun, Y., Feng, H., Manchester, I.R., Yeow, R.C., & Qi, P. (2021). Static Modeling of the Fiber-Reinforced Soft Pneumatic Actuators Including Inner Compression: Bending in Free Space, Block Force, and Deflection upon Block Force. *Soft robotics*.

[2] Carvalho, A.D., NavinKaranth, P., & Desai, V. (2021). Design and characterization of a pneumatic muscle actuator with novel end-fittings for medical assistive applications. *Sensors and Actuators A-physical, 331*, 112877.

[3] Ohta, P., Valle, L.E., King, J.P., Low, K., Yi, J., Atkeson, C.G., & Park, Y. (2018). Design of a Lightweight Soft Robotic Arm Using Pneumatic Artificial Muscles and Inflatable Sleeves. *Soft robotics, 5 2*, 204-215 .

[4] Robinson, R.M., Kothera, C.S., Sanner, R.M., & Wereley, N.M. (2016). Nonlinear Control of Robotic Manipulators Driven by Pneumatic Artificial Muscles. *IEEE/ASME Transactions on Mechatronics, 21*, 55-68.

[5] Ugurlu, B., Forni, P., Doppmann, C., Sariyildiz, E., & Morimoto, J. (2019). Stable Control of Force, Position, and Stiffness for Robot Joints Powered via Pneumatic Muscles. *IEEE Transactions on Industrial Informatics, 15*, 6270-6279.

[6] Zhao, L., Cheng, H., Zhang, J., & Xia, Y. (2021). Adaptive control for a motion mechanism with pneumatic artificial muscles subject to dead-zones. *Mechanical Systems and Signal Processing, 148*, 107155.

[7] Sheikh Sofla, M., Sadigh, M.J., & Zareinejad, M. (2021). Precise dynamic modeling of pneumatic muscle actuators with modified Bouw–Wen hysteresis model. *Proceedings of the Institution of Mechanical Engineers, Part E: Journal of Process Mechanical Engineering, 235*, 1449 - 1457.

[8] Xia, X., & Cheng, L. (2021). Adaptive Takagi-Sugeno fuzzy model and model predictive control of pneumatic artificial muscles. *Science China Technological Sciences*.

[9] Zhao, L., Cheng, H., Xia, Y., & Liu, B. (2019). Angle Tracking Adaptive Backstepping Control for a Mechanism of Pneumatic Muscle Actuators via an AESO. *IEEE Transactions on Industrial Electronics*, 66, 4566-4576.

[10] Huang, J., Cao, Y., & Wang, Y. (2020). Adaptive proxy-based sliding mode control for a class of second-order nonlinear systems and its application to pneumatic muscle actuators. *ISA transactions*.

[11] Ba, D.X., Dinh, T.Q., & Ahn, K.K. (2016). An Integrated Intelligent Nonlinear Control Method for a Pneumatic Artificial Muscle. *IEEE/ASME Transactions on Mechatronics, 21*, 1835-1845.

[12] Qin, Y., Zhang, H., Wang, X., & Han, J. (2022). Active Model-Based Hysteresis Compensation and Tracking Control of Pneumatic Artificial Muscle. *Sensors (Basel, Switzerland), 22*.

[13] Kim, W., Park, H., & Kim, J. (2021). Compact Flat Fabric Pneumatic Artificial Muscle (ffPAM) for Soft Wearable Robotic Devices. *IEEE Robotics and Automation Letters, 6*, 2603-2610.

[14] Petre, I.M. (2021). Studies regarding the Use of Pneumatic Muscles in Precise Positioning Systems. *Applied Sciences*.

[15] Zhao, S., Lei, Y., Wang, Z., Zhang, J., Liu, J., Zheng, P., Gong, Z., & Sun, Y. (2021). Biomimetic Artificial Joints Based on Multi-Material Pneumatic Actuators Developed for Soft Robotic Finger Application. *Micromachines, 12*.

[16] Lolli, V., Rovai, A., Trotta, N., Goldman, S., Sadeghi, N., Lefranc, F., Jousmäki, V., & De Tiège, X. (2021). Pneumatic artificial muscle-based stimulator for passive functional magnetic resonance imaging sensorimotor mapping in patients with brain tumours. *Journal of Neuroscience Methods, 359*.

[17] Tu, Q., Wang, Y., Yue, D., & Dwomoh, F.A. (2020). Analysis on the Impact Factors for the Pulling Force of the McKibben Pneumatic Artificial Muscle by a FEM Model. *J. Robotics, 2020*, 4681796:1-4681796:11.

[18] Wang, X., Yang, L., Sun, Y., & Deng, K. (2017). Adaptive model predictive control of nonlinear systems with state-dependent uncertainties. *International Journal of Robust and Nonlinear Control, 27*, 4138 - 4153.

[19] Hwang, G., Sitapure, N., Moon, J., Lee, H., Hwang, S., & Sang-Il Kwon, J. (2022). Model predictive control of Lithium-ion batteries: Development of optimal charging profile for reduced intracycle capacity fade using an enhanced single particle model (SPM) with first-principled chemical/mechanical degradation mechanisms. *Chemical Engineering Journal*.

[20] Chang, Z., Li, M., Zhu, K.Y., Sun, L., Ye, R., Sang, M., Han, R., Jiang, Y., Li, S., Zhou, J., & Ge, R. (2022). Model predictive control of long Transfer-line cooling process based on Back-Propagation neural network. *Applied Thermal Engineering*.

[21] Dabadghao, V., Biegler, L.T., & Bhattacharyya, D. (2022). Multiscale Modeling and Nonlinear Model Predictive Control for Flue Gas Desulfurization. *Chemical Engineering Science*.

[22] Skupin, P., Laszczyk, P., Goud, E.C., Vooradi, R., & Rao, A.S. (2022). Robust nonlinear model predictive control of cascade of fermenters with recycle for efficient bioethanol production. *Comput. Chem. Eng., 160*, 107735.

[23] Guo, P., Rivera, D.E., Dong, Y., Deshpande, S., Savage, J.S., Hohman, E.E., Pauley, A.M., Leonard, K.S., & Downs, D.S. (2022). Optimizing behavioral interventions to regulate gestational weight gain with sequential decision policies using hybrid model predictive control. *Computers & chemical engineering, 160*.

[24] Johari, S., Yaghoobi, M., & Kobravi, H.R. (2022). Nonlinear model predictive control based on hyper chaotic diagonal recurrent neural network. *Journal of Central South University, 29*, 197-208.

[25] Wu, Z., & Li, Y. (2022). Hybrid Model Predictive Control of Floating Offshore Wind Turbines with Artificial Muscle Actuated Mooring Lines. *Journal of Dynamic Systems, Measurement, and Control*.

[26] Alessio, A., & Bemporad, A. (2009). A survey on explicit model predictive control. *Lecture Notes in Control and Information Sciences*, 345-369.

[27] Bemporad, A., Morari, M., Dua, V., & Pistikopoulos, E.N. (2000). The explicit solution of model predictive control via multiparametric quadratic programming. *Proceedings of the 2000 American Control Conference. ACC (IEEE Cat. No.00CH36334), 2*, 872-876 vol.2.

[28] Grancharova, A., & Johansen, T.A. (2012). Explicit nonlinear model predictive control : theory and applications.

[29] Bemporad, A., Morari, M., Dua, V., & Pistikopoulos, E.N. (2002). The explicit linear quadratic regulator for constrained systems. *Autom., 38*, 3-20.

[30] Wang, X., & Hovakimyan, N. (2012). L1 adaptive controller for nonlinear time-varying reference systems. *Syst. Control. Lett., 61*, 455-463.